Monthly Notices
of the
ROYAL ASTRONOMICAL SOCIETY

Mon. Not. R. Astron. Soc. **421,** 2861–2871 (2012) doi:10.1111/j.1365-2966.2012.20523.x

Simulating protostellar evolution and radiative feedback in the cluster environment

Mikhail Klassen,[1⋆] Ralph E. Pudritz[1,2] and Thomas Peters[3,4]

[1]*Department of Physics and Astronomy, McMaster University, 1280 Main St. W, Hamilton, ON L8S 4M1, Canada*
[2]*Origins Institute, McMaster University, 1280 Main St. W, Hamilton, ON L8S 4M1, Canada*
[3]*Zentrum für Astronomie der Universität Heidelberg, Institut für Theoretische Astrophysik, Albert-Ueberle-Str. 2, D-69120 Heidelberg, Germany*
[4]*Institut für Theoretische Physik, Universität Zürich, Winterthurerstrasse 190, CH-8057 Zürich, Switzerland*

Accepted 2012 January 6. Received 2012 January 6; in original form 2011 November 16

ABSTRACT

Radiative feedback is among the most important consequences of clustered star formation inside molecular clouds. At the onset of star formation, radiation from massive stars heats the surrounding gas, which suppresses the formation of many low-mass stars. When simulating pre-main-sequence stars, their stellar properties must be defined by a pre-stellar model. Different approaches to pre-stellar modelling may yield quantitatively different results. In this paper, we compare two existing pre-stellar models under identical initial conditions to gauge whether the choice of model has any significant effects on the final population of stars. The first model treats stellar radii and luminosities with a zero-age main-sequence (ZAMS) model, while separately estimating the accretion luminosity by interpolating to published pre-stellar tracks. The second, more accurate pre-stellar model self-consistently evolves the radius and luminosity of each star under highly variable accretion conditions. Each is coupled to a raytracing-based radiative feedback code that also treats ionization. The impact of the self-consistent model is less ionizing radiation and less heating during the early stages of star formation. This may affect final mass distributions. We noted a peak stellar mass reduced by 8 per cent from 47.3 to 43.5 $M_\odot$ in the evolutionary model, relative to the track-fit model. Also, the difference in mass between the two largest stars in each case is reduced from 14 to 7.5 $M_\odot$. The H II regions produced by these massive stars were also seen to flicker on time-scales down to the limit imposed by our time-step (<560 yr), rapidly changing in size and shape, confirming previous cluster simulations using ZAMS-based estimates for pre-stellar ionizing flux.

Key words: hydrodynamics – radiative transfer – stars: formation – stars: pre-main-sequence – stars: protostars – H II regions.

1 INTRODUCTION

The conversion of molecular gas into fully formed stars is complex, involving several diverse processes. These different processes are linked to each other through feedback mechanisms that make isolating and understanding the contribution of each process a difficult task. A key point in this regard is that stars also rarely form in isolation, but instead are seen to be forming in clusters and subclusters within molecular clouds (Clarke, Bonnell & Hillenbrand 2000; Testi et al. 2000). In the cluster environment, the formation of a sufficiently massive star can affect all the others through the energy it radiates back into the cloud. Numerical simulations of star formation have made it very clear that the effects of stellar radiation cannot be neglected. Simulations including some form of radiative transfer show a dramatic reduction in the production of brown dwarfs and other low-mass stars (Offner et al. 2009), due to an increase in gas temperatures reducing fragmentation (Krumholz, Klein & McKee 2007; Peters et al. 2010b). More of the available gas mass ends up being accreted by the fewer, larger stars formed, and the fragmentation that does occur takes place in optically thick self-shielding discs (Krumholz et al. 2007; Peters et al. 2010a,b). The fact that radiation affects the mass spectrum in simulations of molecular cloud clumps has obvious implications for the shape of the initial mass function, for example the suppression of excessive brown dwarf formation (Bate 2009; Krumholz et al. 2010; Peters et al. 2010b).

Massive stars also emit prodigious amounts of ultraviolet (UV) radiation (Beuther et al. 2007; Hoare et al. 2007) creating expanding H II regions. The hot (10^4 K) gas expands into the colder (10^2 K) surrounding low-pressure gas, creating another feedback mechanism and ionized region that may contribute to the destruction of molecular clouds (Keto 2002, 2003, 2007; Matzner 2002; Peters et al. 2010a,b). H II regions can be observed by their radio

⋆E-mail: klassm@mcmaster.ca

continuum emission (Mezger & Henderson 1967), or by their recombination lines [e.g. Wood & Churchwell (1989) use the H76α line]. More recently, observations have shown time variability in H II regions (Franco-Hernández & Rodríguez 2004; Rodríguez, Gómez & Tafoya 2007; Galván-Madrid et al. 2008; Gómez et al. 2008). Franco-Hernández & Rodríguez (2004) have suggested that such observed time variability may be due to the changes occurring in the source of the ionizing radiation, though it may also be due to increased absorption in the rapidly evolving core of the nebula. Peters et al. (2010c) present a technique for using synthetic radio maps to study the time evolution of stars forming in a cluster environment and variability in the morphology and size of H II regions. Analysis of these simulations by Peters et al. (2010a) and Galván-Madrid et al. (2011) confirmed variability in the flux and size measurements of H II regions, which in a few cases might be observable on time-scales of $\sim$10 yr. They also noted that positive changes were more likely to occur than negative changes, i.e. that most of the flux variations were increases rather than decreases.

To further explore the impact of radiative feedback and the possible variability in H II regions, simulations must be equipped with good protostellar models. These have been investigated by Palla & Stahler (1991, 1992), Nakano et al. (2000), McKee & Tan (2003), Offner et al. (2009) and Hosokawa & Omukai (2009), among others. It is clear from these models that the evolution of a protostar depends heavily on the mass accretion rate. Among other things, they show that the radius of the protostar may grow or contract depending on the stellar evolutionary stage. With a radius that can change significantly during the pre-main-sequence lifetime of the star, the effective temperature can also be expected to vary significantly. To study this, we simulate the formation of a cluster of stars inside a molecular cloud. We equip the stars with one of two pre-stellar models based on the ones described in Peters et al. (2010a) and Offner et al. (2009), each with its own characteristics. The Offner et al. (2009) model has already been used to study star cluster formation in Krumholz, Klein & McKee (2011), though with different initial conditions. Ours is the first simulation with the protostellar model to also include the effects of ionizing radiation and H II region formation. We connect the model to a radiative transfer method that computes the heating and ionization due to radiation from the stars formed in the simulation.

The differences between the two models are explained in Section 2.1, but the key difference is that the Offner et al. (2009) model treats the evolution of the radius and luminosity self-consistently. The choice of stellar model affects the early evolution of stars in a cluster and may have repercussions for the final mass spectrum. Though not entirely conclusive, we find that reduced heating and ionization in the early stages of star formation when using the Offner et al. (2009) model resulted in a more equitable mass distribution. With the Peters et al. (2010a) model, the cluster came to be dominated more by a single star about 14 $M_\odot$ more massive than the next largest, compared to an $\sim$7.5 $M_\odot$ gap in the Offner et al. (2009) model simulations.

Other effects of the self-consistent pre-stellar modelling are delayed ionization of the cluster gas by 3 per cent of a free fall time (17.7 kyr) and delayed heating of the cluster gas by 1 per cent of a free fall time (5.9 kyr).

Our numerical approach is described in Section 2. In Section 3 we list our results for the early evolution of star clusters with massive stars. We discuss our assessment of the impact of protostellar modelling in Section 4 and summarize our findings in Section 5 with a view to future simulations.

2 NUMERICAL METHODS

We perform numerical simulations using the FLASH hydrodynamics code (Fryxell et al. 2000) in its version 2.5. It is an adaptive-mesh refinement code that solves the gas dynamic equations on an Eulerian grid and includes self-gravity, cooling by dust and by molecular lines (Banerjee, Pudritz & Anderson 2006) and radiative transfer. It has been modified to include Lagrangian sink particles (Banerjee et al. 2009; Federrath et al. 2010) to represent (proto)stars, and a raytracing scheme to handle ionizing and non-ionizing radiation feedback from stars originally developed by Rijkhorst et al. (2006), and then extended and optimized by Peters et al. (2010a). They also tested the code against handling a D-type ionization front, comparing it to the approximate solution found by Spitzer (1978), while the code's ability to handle R-type ionization fronts had already been tested by Iliev et al. (2006). Accretion rates on to sink particles are calculated based on a single time-step. FLASH does not have adaptive time-steps, so every refinement level advances with the same time-step.

The opacities for the non-ionizing radiation are the same as in Peters et al. (2010a). We use *Planck* mean opacities as interpolated from the Pollack et al. (1994) data by Krumholz et al. (2007). They assume that the radiation temperature is equal to the gas temperature because their core is optically thick. We make the same approximation using the assumption that the star will be embedded in an (unresolved) dense envelope of gas through which the stellar radiation must propagate before entering the scales of our simulation, thereby changing its spectrum accordingly.

We subsequently added an additional module to handle the protostellar evolution of our sink particles, which is based on a subgrid physics model described in detail in Offner et al. (2009). The protostellar model connects directly to the radiation module so that stellar surface temperatures and stellar radii are handled self-consistently.

We perform two comparison simulations, each with a different prestellar model, the initial conditions of which are summarized in Table 1.

2.1 Protostellar models

The radiative feedback model is coupled directly to the sink particles. Rays are cast outwards from each sink particle and the column density along each ray is computed using the hybrid-characteristics scheme described in Rijkhorst et al. (2006). At each cell in the computational domain, the photoionization rate and heating rate are calculated. These are set by the specific mean intensity along the ray,

$$J_\nu(r) = \left(\frac{r_{\rm star}}{r}\right)^2 \frac{1}{2c^2} \frac{h\nu^3 \exp\left[-\tau_{\rm ion}(r)\right]}{\exp(h\nu/k_{\rm B}T_{\rm star}) - 1}, \quad (1)$$

which depends on the knowledge of the radius of the star $r_{\rm star}$.

The stellar radius depends on the choice of stellar model. The simplest stellar model would be to assume that all stars are zero-age main-sequence (ZAMS) stars and use a lookup table, such as the one by Paxton (2004), to retrieve the radius for a star residing in a particular mass bin of the table. Such a table will also contain surface effective temperatures for ZAMS stars. The intrinsic stellar luminosity is then found from $L_{\rm int} = 4\pi R_*^2 \sigma T_{\rm eff}^4$. This model may be acceptable for most circumstances, but breaks down for when attempting to model pre-main-sequence stars. If one treats these low-mass stars as ZAMS stars, the model will underestimate their radii and overestimate their surface temperatures. It will also lead to an overestimation of the accretion luminosity $L_{\rm acc} = GM\dot{M}/R$.

Table 1. Runtime parameters of the clustered star formation simulations.

Run	Mass	Density profile	Temperature	Rotation	Stellar model	Feedback
1	$1000\,\mathrm{M}_\odot$	$r^{-3/2}$	30 K	$\beta = 0.05$	'Evolving protostars'	Radiative; raytracing method
2	$1000\,\mathrm{M}_\odot$	$r^{-3/2}$	30 K	$\beta = 0.05$	'Augmented ZAMS'	Radiative; raytracing method

In Peters et al. (2010a), a kind of 'augmented ZAMS' model is used, which we will refer to as A-ZAMS throughout the paper. This pre-stellar model uses a ZAMS description as detailed above when calculating the stellar radius and intrinsic luminosity of stars. To avoid overestimating the accretion luminosity, a separate accretion radius is calculated. This is achieved by referencing the pre-main-sequence tracks computed by Hosokawa & Omukai (2009) for mass accretion rates between 10^{-6} and $10^{-3}\,\mathrm{M}_\odot\,\mathrm{yr}^{-1}$ and then interpolating between them based on the current mass accretion rate for the star. The advantage of this model is that it is relatively straightforward to implement and prevents grossly overestimating the accretion luminosity, which dominates the total luminosity of a star during its early lifetime. The disadvantage of this model is that it is not self-consistent and relies on two separate radii being computed or retrieved from a table. The accretion radius, found by interpolation to tracks of constant accretion rate, is sensitive to fluctuations of the accretion rate. A rapidly fluctuating accretion rate means the accretion radius will fluctuate with equal rapidity – and unphysical consequence.

An alternative approach is to use the self-consistent evolving protostellar model developed by Tan & McKee (2004) and described in detail in Offner et al. (2009). Stars are modelled as polytropes and every sink particle in our simulation is assigned several additional properties: a stellar radius r_{star}, an intrinsic luminosity L_{int}, a polytropic index n, an unburned deuterium mass m_{d} and a nuclear burning evolutionary stage. At every time-step in our simulation, we evolve this handful of variables according to the equations given in Offner et al. (2009). The model is based on a one-zone protostellar evolution model introduced by Nakano, Hasegawa & Norman (1995) and further developed by Nakano et al. (2000) and Tan & McKee (2004).

We refer to this pre-stellar model as the 'evolving protostar' model, to distinguish it from the A-ZAMS model employed in Peters et al. (2010a) and used for comparison here. It is so called because the stellar properties are co-evolved with the rest of the simulation instead of calculated on the fly.

When a sink particle's mass exceeds $0.1\,\mathrm{M}_\odot$, we activate our protostellar evolution code and initialize the radius and polytropic index, respectively, as

$$r = 2.5\,\mathrm{R}_\odot \left(\frac{\Delta m/\Delta t}{10^{-5}\,\mathrm{M}_\odot\,\mathrm{yr}^{-1}} \right)^{0.2} \tag{2}$$

$$n = 5 - 3\left[1.475 + 0.07\,\log_{10}\left(\frac{\Delta m/\Delta t}{\mathrm{M}_\odot\,\mathrm{yr}^{-1}} \right) \right]^{-1}. \tag{3}$$

For cool stars, the Hayashi limit sets the luminosity, but above this a main-sequence luminosity is assumed. Thus, $L_{\mathrm{int}} = \max(L_{\mathrm{H}}, L_{\mathrm{ms}})$, with $L_{\mathrm{H}} = 4\pi R^2 \sigma T_{\mathrm{H}}^4$ and $T_{\mathrm{H}} = 3000\,\mathrm{K}$. ZAMS values for the radius and luminosity are computed using the fitting formulae by Tout et al. (1996).

Apart from initializing our model at a higher starting mass, the only other significant difference is that we take accretion luminosity to be $L_{\mathrm{acc}} = GM\dot{M}/R$. The evolving protostar model treats accretion on to the disc, with an associated luminosity of $L_{\mathrm{disc}} = (1/2)\,GM\dot{M}/R$ (standard for an alpha disc), and surface accretion, with luminosity $L_{\mathrm{acc}} = (1/4)\,GM\dot{M}/R$. This is due to the assumption that some of the energy is being used to drive a wind. We do not make this assumption. We also rely on tables of polytropic stellar parameters that we computed ourselves. In all other respects, our protostellar model follows the one described in Offner et al. (2009).

Protostars evolve through multiple distinct nuclear stages in this code during which the radius is at times expanding (such as during the early accretion phase) and at times contracting (such as during the end stage as the protostar approaches the main sequence to be a mature star). Once our stars reach the main sequence, we assign them a radius and luminosity based on the fitting formulae of Tout et al. (1996). We neglect any special treatment of metallicity-related effects and consider only stars of solar metallicity.

To compute the ionizing flux, we take the stellar radius and surface temperature from either a table of ZAMS values (in the case of the A-ZAMS model) or read the current, evolved values from the sink particle properties computed by the protostellar code (in the case of the evolving protostar model). The flux of ionizing photons is computed by integrating the Planck function above the threshold frequency for hydrogen ionization. The radiative feedback code computes gas heating considering both the intrinsic and accretion luminosities.

This protostellar evolution code is a one-zone model that upgrades the current treatment of sink particles in FLASH and is a more accurate representation of pre-main-sequence stars. In Figs 1 and 2 we compare the results of this model with the stellar structure

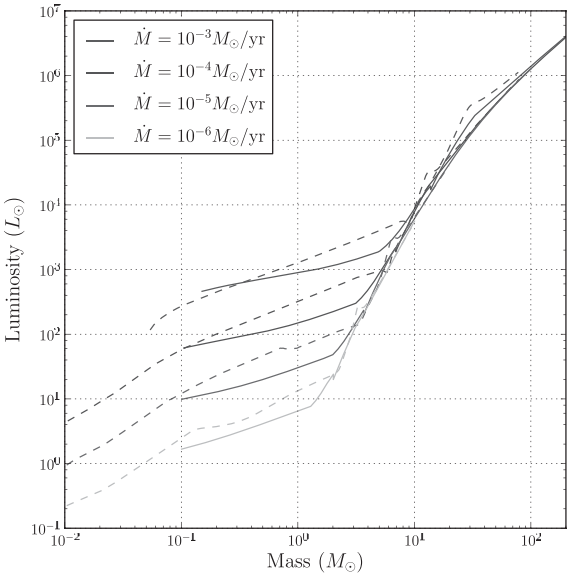

Figure 1. Luminosity evolution for protostars accreting mass at various rates. The solid lines show the intrinsic (stellar) luminosity following the evolving protostar model, whereas the dashed lines show the luminosity derived from stellar structure modelling by Hosokawa & Omukai (2009).

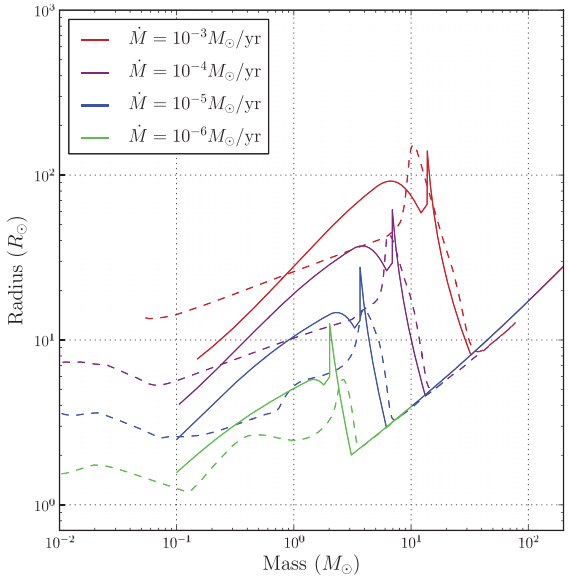

Figure 2. Mass–radius relation for accreting protostars. The solid lines show the stellar radius following the evolving protostar model, whereas the dashed lines show the radius derived from stellar structure modelling by Hosokawa & Omukai (2009). The one-zone model approximates the stellar structure results to within a factor of ∼2.

modelling of Hosokawa & Omukai (2009), which is expected to be more accurate than one-zone modelling.

We compare the behaviour of our code at different accretion rates ranging between a slow 10^{-6} and a rapid $10^{-3}\,\mathrm{M}_\odot\,\mathrm{yr}^{-1}$. These represent the typical range of accretion rates we see in our simulations and expect of stars forming in clusters within molecular clouds. The stability of the code was tested over a range of accretion rates and time-step sizes. Although our tracks do not agree perfectly with the Hosokawa & Omukai (2009) simulations, the agreement is to within a factor of ∼2.

Table 2, with its accompanying Fig. 3, summarizes what is described in detail in the appendices of Offner et al. (2009).

2.2 Initial conditions

The strength of the radiative feedback code we employ lies in its ability to produce realistic H II regions. It was believed, however, that since the radius and stellar luminosity of young protostars are represented by ZAMS-equivalent values in Peters et al. (2010a), the ionizing flux would be overestimated. To study whether this was indeed the case, and also what impact a different pre-stellar model would have generally, we simulated a collapsing molecular cloud clump with each of the two pre-stellar models.

In the first case, we chose to repeat the cluster simulations described in Peters et al. (2010a) with similar initial conditions, but at a slightly lower resolution. Because we use the same FLASH code, sink particles and radiative feedback code, we can isolate the effect of including a protostellar evolution model. We begin with a $1000\,\mathrm{M}_\odot$ self-gravitating clump of molecular hydrogen at an initial temperature of 30 K. The cloud is in solid body rotation with a ratio of rotational to gravitational energy of $\beta = 0.05$. Our simulation box is 3.89 pc on a side. At maximal refinement, the grid size is 196 au. The density profile features a flat central region extending out to a radius of 0.5 pc and then falling off according to an $r^{-3/2}$ power law. The central density is $\rho_\mathrm{c} = 1.27 \times 10^{-20}\,\mathrm{g\,cm^{-3}}$. The density drops off until reaching an ambient cut-off density of $\rho_\mathrm{ext} \approx 9.76 \times 10^{-23}\,\mathrm{g\,cm^{-3}}$. Sink particles have a radius of 1175 au, or six times the grid size at maximal refinement. The cut-off density for sink particle creation is $4.4 \times 10^{-17}\,\mathrm{g\,cm^{-3}}$.

We note that clumps of this size and mass are expected to be turbulent (Blitz 1993; Evans 1999; Williams, Blitz & McKee 2000). However, in order to build up physical understanding of the complex process of cluster formation, we follow Peters et al. (2010a) in this

Table 2. Description of the stellar evolutionary stages in the evolving protostar model.

	Stage	Features
0	Pre-collapse	Mass $m \lesssim 0.1\,\mathrm{M}_\odot$ Cannot dissociate H_2 and cause second collapse to stellar densities
1	No burning	Object has collapsed to stellar densities T_c still too cold to burn D $T_\mathrm{c} \lesssim 1.5 \times 10^6$ K Radiation comes purely from gravitational contraction Star is imperfectly convective
2	Core D burning at fixed T_c	Temperature reaches required $T_\mathrm{c} \sim 10^6$ K to burn deuterium D burning acts as a thermostat keeping temperature constant Star is fully convective
3	Core D burning at variable T_c	D is exhausted Core temperature now rising again Star remains fully convective Accreted D dragged down to core and burned Rising core temperature reduces opacity Convection in the stellar core eventually shuts down
4	Shell D burning	Star core changes to a radiative structure, swelling the radius D burns in a shell around the core After initial swelling, radius contracts down to a ZAMS radius
5	Main sequence	Star has contracted enough for T_c to reach $\sim 10^7$ K Hydrogen ignites and star stabilizes on to the main sequence

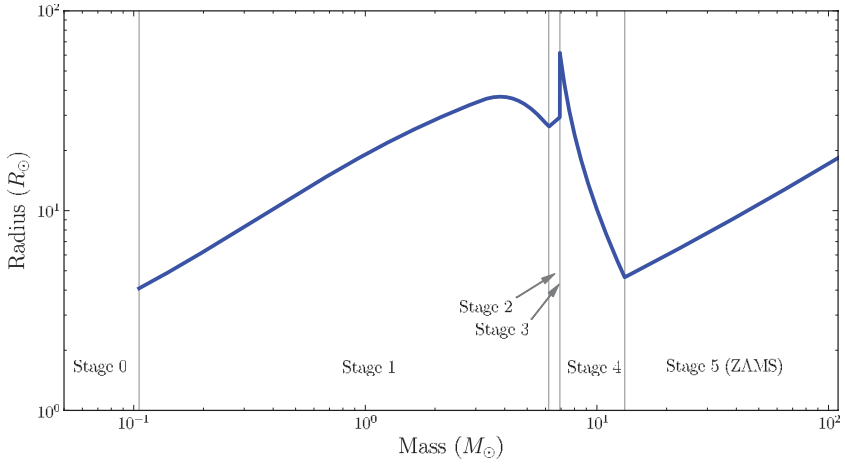

Figure 3. Radius evolution of a star accreting at a steady $10^{-3}\,M_\odot\,yr^{-1}$ under the protostellar model of Offner et al. (2009) with stages outlined in Table 2.

study and ignore turbulence so that we can isolate the important radiative feedback effects. Turbulence will be added in subsequent papers.

We show the results of two of our simulations: one using the A-ZAMS approach for stellar effective temperature and stellar radius, and a second with the evolving protostellar model.

As the simulation progresses, the original mass profile of the clump quickly disappears as it undergoes gravitational collapse to produce a rotating central disc. Stars, represented by sink particles, are allowed to form when the local conditions satisfy the criteria described in Federrath et al. (2010).

3 STAR FORMATION AND FEEDBACK IN THE CLUSTER ENVIRONMENT

We investigate what difference protostellar modelling makes to the overall evolution of the cluster. The most important consequence of the improved hybrid characteristics raytracing code employed by Peters et al. (2010a) is that it allows for the realistic simulation of H II regions, with ionization, heating and shadowing effects built in. One of the most important consequences of accurate pre-main-sequence modelling is that it tempers the ionization and heating in the early stages of star formation.

To study this effect, we look at two variables: mean ionization in our simulation box and mean gas temperature. Fig. 4 shows these two measurements as functions of time in our simulation. Time is measured in units of global free fall time, or $t_{\rm ff} \approx 590\,000$ yr. With the model of Peters et al. (2010a), sink particles follow a ZAMS model for the stellar radius and intrinsic luminosity, which means that they are hotter and more compact than true pre-main-sequence stars. This causes them to release more ionizing photons, compared to the protostellar case. The onset of ionization in this case leads the evolving protostar case by about 0.03 free fall times, or about 17.7 kyr. The onset of star formation in both simulations occurs at around 1 free fall time. For both cases, after 1.1 free fall times, the largest star in either simulation is at $\sim 20\,M_\odot$ and dominates the UV output of the cluster, resulting in comparable mean ionization for both cases.

When we consider mean temperature instead of mean ionization, the leading effect by the ZAMS-based model is still there, only less pronounced. Major heating of the gas in this case leads to the evolving protostar model case by close to 0.01 free fall times, or about 5.9 kyr. The first star to form in a cluster tends to grow to be among the largest stars in the cluster and dominate the heating and ionization. This suggests that accurate protostellar modelling is most important in the early stages of a cluster simulation, and for low-mass stars. Offner et al. (2009) showed that radiation even from low-mass stars has a significant effect on the gas heating and formation of brown dwarfs.

To get a visual sense of the gas dynamics and configuration of the cluster, we visualize the gas density by taking slices through our simulation box. Zoomed-in views of the cluster are shown in Fig. 5. The simulation box is actually about 3.8 pc across. Here we show the central region at about 0.5 pc across. The upper row in the figure

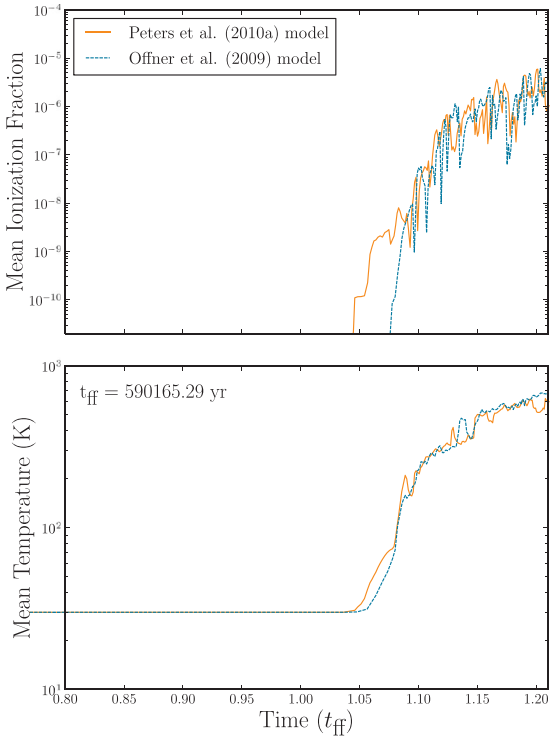

Figure 4. A comparison of the mean ionization fraction and mean temperature in cluster simulations with different pre-stellar models. In each case, the mean is calculated by finding the volume-weighted average. Values are only meaningful in a relative sense, as the simulation volume is large (side length ~3.8 pc) and the most active region is the inner cubic parsec.

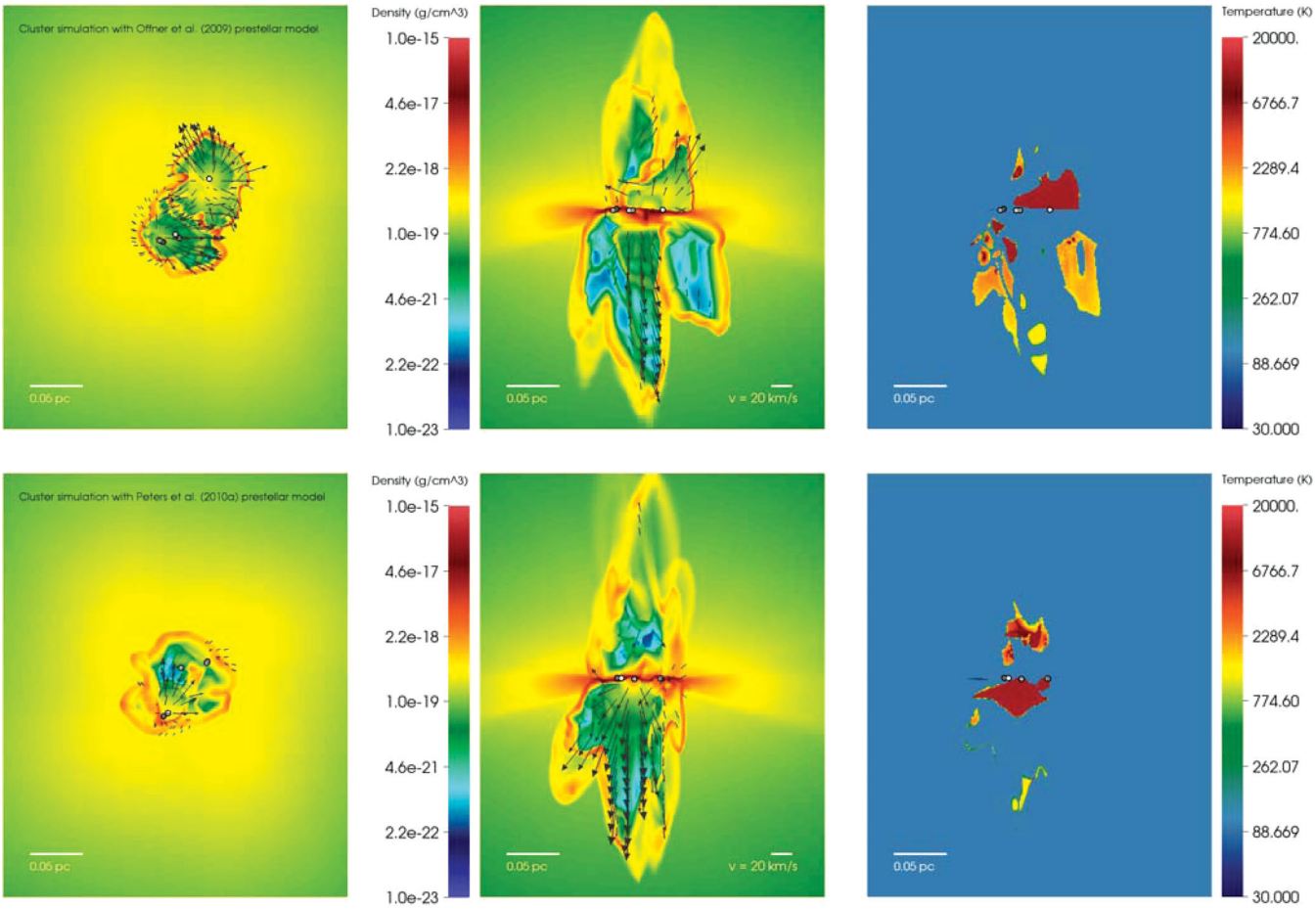

Figure 5. The two rows show the results from the two pre-stellar models tested, with the A-ZAMS model of Peters et al. (2010a) in the top row and the evolving protostar model of Offner et al. (2009) in the bottom row. Each is shown near the end of the simulation, after about 1.21 free fall times (714 kyr). In each row, the panels show, from left to right, the gas density in a horizontal slice through the mid-plane, the gas density in a vertical slice in the centre of the simulation box and the gas temperature in the same slice. Scale bars indicate the physical sizes and the speeds represented by vectors in the gas density panels. The scale for these vectors is the same for both side views and top–down views. Stars are indicated by black circles. The online version of this paper includes movies of the time evolution of gas density and ionization fraction – see supporting information.

shows the simulation results with the evolving protostar model, while the lower row shows the A-ZAMS results. In each row, the panels show gas density in a horizontal slice through the mid-plane of the simulation box (left), gas density in a vertical slice showing the cluster edge-on (centre) and gas temperature in the same vertical slice (right). Gas temperature is discussed in Section 3.4. The two density panels also show velocity vectors for the high-velocity gas. The fastest moving gas travels at close to 30 km s^{-1}. Gas densities range from 10^{-23} to 10^{-15} g cm^{-3}. The hollowed-out H II regions, where the gas is largely ionized, expand outwards above and below the disc as a kind of fountain before falling back on to the disc.

Sink particles indicating the locations of stars are marked with black-rimmed grey points. The side view shows the stars to be confined to the disc while the top–down shows the stars packed in a tight cluster. The separation between stars nowhere exceeds 0.1 pc. During the course of the simulation, stars are seen to be dynamically interacting, exchanging angular momentum, forming and breaking apart binaries.

These snapshots of the simulation are taken at around 1.21 free fall times in each case, near the end of the simulation. At this stage, about 714 kyr have elapsed since the beginning of the simulation, with the onset of star formation having occurred at around 600 kyr. At this stage, both model results look similar in many ways: the stars are in a densely packed cluster, and each cluster has produced an expanding H II region. The H II regions in each figure are approximately the same size, although amorphous and variable. They do not seem to be affected by our choice of pre-stellar model. This is because of how each cluster has become dominated by massive stars already evolved on to the main sequence, and the differences between pre-stellar models have vanished. The stars are all releasing copious amounts of ionizing radiation, driving the evolution of these H II regions.

3.1 Binaries

Zinnecker & Yorke (2007) state that massive stars occur more frequently in binaries relative to low-mass stars. Lacking turbulence and magnetic fields, our molecular gas clumps do not represent the true initial conditions for cluster formation, but the stars in our simulations to form binaries. There is no reason to suspect that the choice of protostellar model has any effect on binary formation or binary mass ratios. Lacking ensemble averages, we cannot make any special claims, but report that of the five stars formed in each of our simulations, four stars end up in binaries. Dynamical encounters

Table 3. Final stellar masses after 1.21 free fall times (714 kyr) in each cluster simulation, in units of solar masses, comparing the different pre-stellar model results.

Evolving protostars	Augmented ZAMS
43.5	47.3
36.0	33.3
28.5	28.4
22.3	17.3
7.6	14.0

between stars cause binaries to form, break apart and reform. The final mass ratios of the two pairs in each simulation were 3.74 and 1.61 with the Offner model. The Peters model simulation showed mass ratios of 3.38 and 1.92. The final masses of the stars formed in each simulation are reported in Table 3.

3.2 Accretion histories

We now compare the simulations with a focus on the accretion histories of the sink particles. Peters et al. (2010a) have shown that the gas surrounding the centre of the cluster would fragment and result in a highly variable accretion rate. We see this in Figs 6 and 7, where we show in the two panels the accretion histories of every sink particle formed in our simulation along with their accretion rates.

In the lower panel we see the accretion rate of each star, and for most of the stars in our simulation, the accretion rate remains between 10^{-4} and $10^{-3}\,\mathrm{M}_\odot\,\mathrm{yr}^{-1}$.

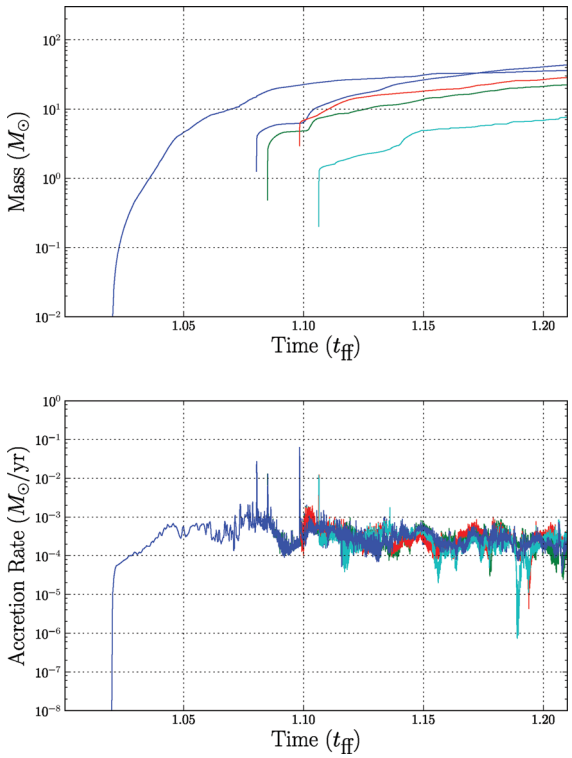

Figure 6. Accretion histories of stars formed in the cluster simulation of the evolving protostar setup. The upper panel shows the mass of each particle as a function of time. The lower panel shows the accretion rate in units of $\mathrm{M}_\odot\,\mathrm{yr}^{-1}$ as a function of time. The dynamical time is about 0.59 Myr.

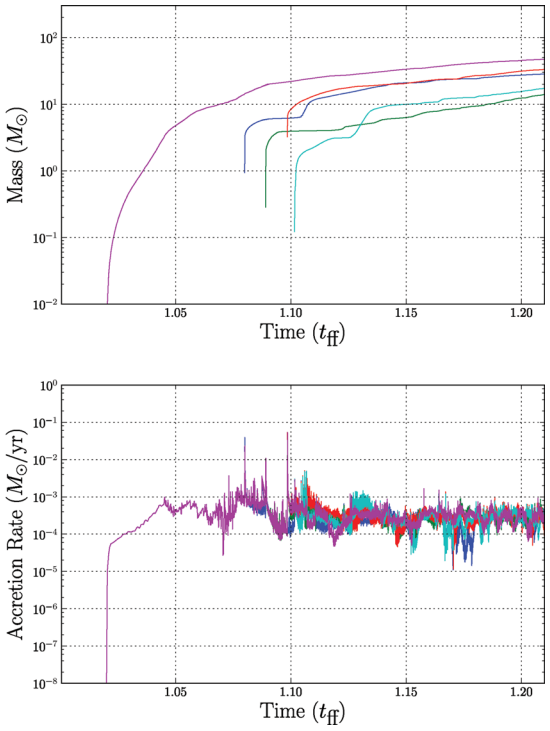

Figure 7. Accretion histories of stars formed in the cluster simulation of the A-ZAMS setup. The upper panel shows the mass of each particle as a function of time. The lower panel shows the accretion rate in units of $\mathrm{M}_\odot\,\mathrm{yr}^{-1}$ as a function of time. The dynamical time is about 0.59 Myr.

The upper panel in Fig. 6 shows the growing masses of each of the stars in our protostellar model simulation. Star formation does not really commence until after the first dynamical time (free fall time) – about 0.59 Myr for our simulation setup. There seems to be a burst of star formation after $t \approx 1.10 t_{\rm ff}$. Interestingly, the most massive star is not the first star in our simulation, but it is overtaken in mass by the second star, which reaches a final mass of about $43.5\,\mathrm{M}_\odot$. The others reach final masses of approximately 36.0, 28.5, 22.3 and 7.6 $\mathrm{M}_\odot$. The average mass of these five stars is 27.6 $\mathrm{M}_\odot$. We were able to run the evolving protostar simulation longer than the A-ZAMS case. During this extra time, three additional stars formed and accreted about $1\,\mathrm{M}_\odot$ of material each, but we do not use this additional data in our comparison with the A-ZAMS case.

In the A-ZAMS case, shown in Fig. 7, the final masses of the stars are 47.3, 33.3, 28.4, 17.3 and 14.0 $\mathrm{M}_\odot$. The average mass of these five stars is 28.1 $\mathrm{M}_\odot$. It is difficult to draw firm conclusions about the impact of a protostellar model on the population dynamics of a cluster. We would need to complete longer simulations under more realistic initial conditions (including turbulence). The evolving protostars run experienced a second wave of star formation, but when we restrict ourselves to comparing only the first $1.21 t_{\rm ff}$ in each case, we find that they have almost the same average mass.

Interestingly, though, the evolving protostar case had four stars with masses greater than $10\,\mathrm{M}_\odot$. These were all more closely packed (smaller variance) than the four most massive stars in the A-ZAMS case. We propose that the reduced initial heating and ionization from the self-consistently evolved pre-main-sequence stars results in a more equitable partition of mass between the massive stars. The most massive star in this simulation outranks the second largest by about $7.5\,\mathrm{M}_\odot$. By comparison, the leading star in the A-ZAMS simulation exceeded the next most massive star by

14 $M_\odot$, or nearly double. Further simulations with different initial conditions are required to confirm whether this choice of pre-stellar model will always have such an impact.

These are the results of only a single simulation in each case, so it is difficult to say that this difference in massive spectrum is highly significant, especially given that the average mass of each cluster is similar and our simulations did not contain turbulence. By other measures, such as the average ionization, mean temperature or H II region morphology, the two pre-stellar models converged and gave similar results. The mass spectrum shows a similar average mass of ∼28 $M_\odot$, but with the evolving protostar model having both a smaller peak mass and smaller difference in mass between the two top stars relative to the A-ZAMS model.

We were able to run the protostellar simulation a little longer than the A-ZAMS simulation; there occurred a second burst of star formation that only appeared very late in the simulation. These stars grew to be 1.9, 1.3 and 1.0 $M_\odot$. The A-ZAMS run may have formed more stars if run for longer. We have run each setup for approximately two weeks on 64 processors, or approximately 21 500 CPU-hours. The protostellar simulation progressed further than the ZAMS simulation. In either case, memory or eventual code stability limited the length of the runs.

3.3 Mass–radius relation

The mass–radius relation for a star is a means of comparing different protostellar models. It is also a way of seeing the evolution of the stars in our simulation. As stars accrete mass or undergo nuclear-structural changes in their interiors, the radius reacts either by expanding or contracting. We see the evolution of the stars in our simulation represented in Fig. 8. In this figure we compare the radii of stars from our different cluster simulations.

We show the accretion radius for a single star in the A-ZAMS run by the grey line in Fig. 8. The red lines in this figure are the stars following the protostellar evolution model that we have described in Section 2.1. These stars have their radius continuously evolved according to their burning state and the accretion of new material. The radius, therefore, does not fluctuate with unrealistic rapidity. Because the model has a self-consistent description of the radius, we use the same quantity to describe the stellar radius and the accretion radius, rather than computing each by different means.

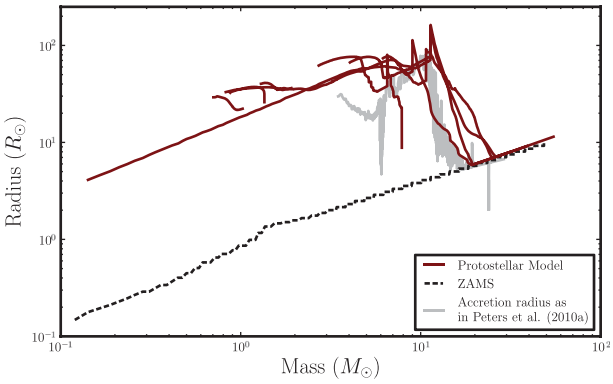

Figure 8. The mass–radius relation for the stars in both cluster simulations. The black dashed line marks the stellar radius track of sink particles in the A-ZAMS simulation. The radius is based on tabulated values of luminosities and temperatures for ZAMS stars. The grey line indicates the separately calculated accretion radius for a single star. The red lines mark the tracks of sink particles following the evolving protostar model. This protostellar radius is used as both the stellar radius and the accretion radius.

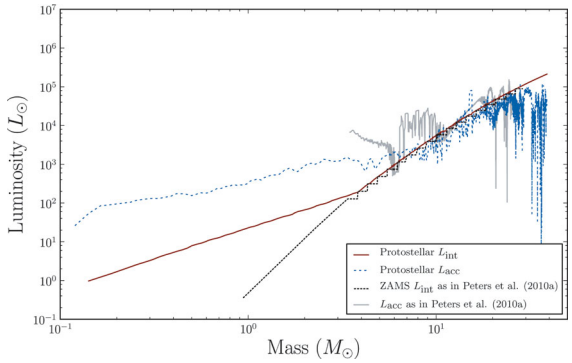

Figure 9. The mass–luminosity relation for a representative star in each of the two cluster simulations. For each star, its accretion luminosity and intrinsic stellar luminosity are plotted. The red and dashed blue lines show the intrinsic stellar luminosity and the accretion luminosity, respectively, of a star in the evolving protostar simulation. The black dashed line, with its stepped appearance, represents the intrinsic luminosity of a ZAMS star, retrieved from a table of ZAMS values. Finally, the grey line shows the accretion luminosity of a star in our A-ZAMS simulation. The luminosity is calculated as in Peters et al. (2010a) by an interpolation of the radius to models by Hosokawa & Omukai (2009).

Protostars have radii an order of magnitude larger than a ZAMS star of equal mass. Hence, their effective temperatures and flux of ionizing photons are going to be much less (for a 1 $M_\odot$ star, 3000 K versus 5000 K in effective temperature, 10^{29} s^{-1} versus 10^{39} s^{-1} in ionizing photons). A star in simulations without protostellar modelling may excessively heat or ionize the gas during the early phases of star formation.

The evolution of the stars in each simulation is also revealed by the mass–luminosity relation, shown in Fig. 9. The black and grey lines belong to a representative star in the A-ZAMS model simulation, and dark red and blue to a representative star in the protostellar simulation. The accretion luminosity, calculated as $L_{\rm acc} = GM\dot{M}/R_{\rm acc}$, is especially sensitive to the accretion rate $\dot{M}$ and the accretion radius $R_{\rm acc}$. The stars show accretion luminosities that are up to an order of magnitude larger than the stars in the evolving protostar model simulation on account of the difference in stellar radius. Only for stars larger than about 20 $M_\odot$ do the differences between the two models disappear. The black jagged line indicates the main-sequence luminosities from a pre-computed table, which tends to underestimate stellar luminosities for protostars less than about 3 $M_\odot$. The protostellar luminosity of one star is given by the dark red line and the protostellar accretion luminosity by the blue line. Much of the rapid fluctuation in the accretion luminosities of both simulations stems from the highly variable mass accretion rate (see Figs 6 and 7).

3.4 Ionization and temperature

Protostars have large radii about an order of magnitude larger than equivalent-mass main-sequence stars. They may be just as luminous, and they certainly have high accretion luminosities, but it is the effective temperatures of their surfaces that determine how great the flux of ionizing photons will be, if the star emits any at all. The single greatest difference we see when simulating the evolution of a star cluster with self-consistent protostellar modelling is that when the first stars begin to form after about a dynamical time, the average gas temperature and average ionization of the gas are considerably less in the simulation involving our protostellar model (Fig. 4).

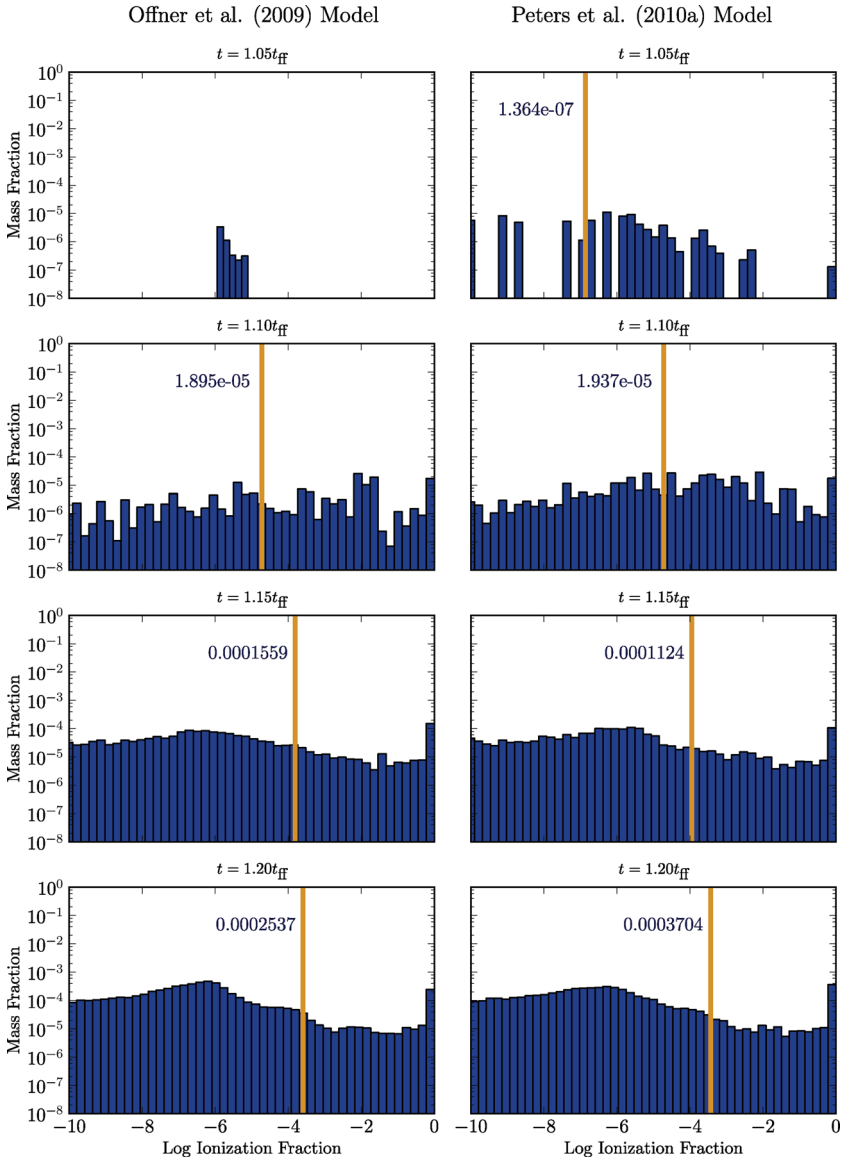

Figure 10. The evolving mass-weighted ionization fraction spectrum. Compared are cluster simulations with stars running on the evolving protostar model of Offner et al. (2009) in the left-hand column and the A-ZAMS model of Peters et al. (2010a) in the right-hand column. A distribution of the total mass in the simulation box (about 1000 $M_\odot$) is shown for $t = 1.05, 1.10, 1.15, 1.20t_{\rm ff}$. One free fall time is approximately 0.59 Myr. The yellow line indicates the mass-weighted average ionization fraction, the numerical value of which is printed to the left of the line.

Fig. 10 shows the mass-weighted spectrum of the ionization fraction in both cases, with the evolving protostar model on the left and the A-ZAMS model on the right. Values for ionization fraction range from 10^{-10} to approximately 1 (completely ionized). Ionization fractions $\ll 1$ should not be taken too seriously, as our model includes only stellar ionizing radiation from the stars in our cluster. The figure shows the spectrum for all the gas involved in the simulation – approximately 1000 $M_\odot$ in total. The thick yellow line indicates the mass-weighted average value for the ionization fraction with the value printed beside the line. Individual snapshots in time are $t = 1.05, 1.10, 1.15$and$1.20t_{\rm ff}$.

It is important to show how the averages change over time in Fig. 4 because of how the mean tends to fluctuate yet the two models have similar values for all but the earliest phases of star formation. The early phase is shown in the first row, at $t = 1.05t_{\rm ff}$. Here there is a significant difference in the mean ionization fractions of the two models. The low-mass ZAMS stars are hotter and have smaller radii. There is greater early ionization seen in this case. At later stages, the distributions appear more similar as the conspicuous effects of the model disappear.

The temperature structure of the gas surrounding the cluster is shown in the right panels of Fig. 5. These reveal some interesting features. The gas in the vicinity of the cluster is approximately 100 K, heating to this temperature by the non-ionizing radiation coming from the cluster. We also see pockets of very hot (10^4 K) ionized gas in the expanding H II regions. When we study the evolution of these regions in time, we see that these pockets of high-temperature gas are very transient: forming, expanding, breaking apart and cooling very rapidly. They are due to photoionization and photoionization heating caused by the massive stars in the cluster. Peters et al. (2010a) have attributed this flickering to the chaotic gas motions in the cluster. Gas moves towards the interior of the cluster through the disc and interacts with the ionizing radiation giving rise to many unstable morphologies that expand outwards above and

below the disc. This has the appearance of flickering on relatively short time-scales: less than 560 yr – the temporal resolution of our simulations. Synthetic observations of the original Peters et al. (2010a) results analysed by Galván-Madrid et al. (2011) have revealed this flickering visible in radio-continuum emission and have demonstrated that it is in agreement with available observations.

4 DISCUSSION

Considering that the radii and luminosities of true protostars are vastly different from their ZAMS counterparts (i.e. Figs 8 and 9), it may seem surprising that our two simulations actually look so alike. For instance, the two simulations form an equal number of stars, their average mass is approximately the same and morphology of the clump with its outflows and H II regions appear qualitatively similar in both cases. It is important to note what we are comparing. The model that we are comparing against Peters et al. (2010a) treated the stellar radius and the accretion radius separately, meaning that gas heating has two components: one due stellar radiation and one due to the accretion luminosity. The mass–luminosity relation of Fig. 9 shows that the ZAMS stellar luminosity underestimates the true protostellar luminosity for pre-main-sequence stars. It also shows that the accretion luminosity, calculated as in Peters et al. (2010a) by an interpolation to the Hosokawa & Omukai (2009) models, overestimates the true protostellar accretion luminosity. So there are two competing differences and these effects will partially cancel each other out. The result is that our evolving protostar simulation looks similar in many ways to the results of Peters et al. (2010a). If Peters et al. (2010a) had not boostrapped the separate treatment of accretion radius on to the ZAMS model, there may have been a gross overestimation of the accretion luminosity – which dominates the total luminosity of a star during its early lifetime. The errors resulting from this overestimation could be substantial.

In our radiative feedback technique, we treat ionization separately from heating, and ionization depends solely on the effective temperatures of our stars. Since protostars have cooler surface temperatures than ZAMS stars of equal mass, there is much less early ionization. Since it is the ZAMS stars of high mass that dominate the radiation output of a cluster, the differences between our model and the ZAMS model disappear after the early stages of stellar evolution (Fig. 10). A side-by-side comparison of the ionizing flux from stars with different stellar models will be included in a forthcoming paper.

Our simulations have a number of limitations that should be noted. They neglect the effects of radiation pressure. On large scales, radiation pressure from stellar clusters could drive galactic winds (Murray, Ménard & Thompson 2011). However, within our low-density $1000\,M_{\odot}$ cluster, radiation pressure below the Eddington limit should not be dynamically significant (Yorke & Sonnhalter 2002; Krumholz & Matzner 2009). After the first absorption/re-emission event, the radiation will have been converted to infrared radiation to which the molecular cloud is largely transparent. The first absorption event is unlikely to impart a significant amount of momentum.

In our simulations, we have treated gas that was initially cold and in solid body rotation, but without any turbulence. Cluster-forming clumps in molecular clouds are observed to have supersonic turbulence, and a more realistic set of initial conditions would include turbulence. However, this might have obscured the effects of our protostellar model that we were seeking to measure. We are currently preparing to run simulations that include realistic turbulent initial conditions as well magnetic fields, which were also left out of this simulation [see, however, Peters et al. (2011) for the effects of magnetic fields on our non-turbulent initial conditions].

The protostellar model we have added to our simulations improves on previous work by adjusting the ionizing luminosity so that it matches the stellar surface effective temperatures for accreting protostars, which initially have radii larger than equal-mass stars on the main sequence. We note, however, that a full-spectrum treatment of the radiation still faces technical and computational limits that make the problem extremely challenging. As a compromise, we break the radiation into its ionizing and non-ionizing components.

5 CONCLUSIONS

Stars begin to affect their birth environments as soon as they are born through radiative feedback. We have considered the impact that pre-main-sequence modelling can have on a star cluster by comparing two different pre-stellar models already described in the literature. We did this by repeating the simulation of Peters et al. (2010a). We then upgraded the FLASH code to include a protostellar evolution module based on the one described in the appendices of Offner et al. (2009).

Each model works by equipping the stars in the simulation ('sink particles') with a stellar radius and luminosity. The greatest difference between the two models was self-consistency. The Peters et al. (2010a) model calculated approximate stellar parameters on the fly, while the evolving protostar model evolved the stellar parameters self-consistently through the simulation as the stars grew and accreted mass.

In terms of the overall gas structure, H II regions, temperature structure, mean ionization fraction or stellar binarity, the two models produced qualitatively the same results. This is because a cluster comes to be dominated by its most massive stars, which are evolved, main-sequence, highly luminous stars, regardless of the choice of stellar model. These one or two massive stars control the overall dynamics.

The differences exist in the early phase of star formation. Major ionization of the gas in the evolving protostar model lagged the Peters et al. (2010a) model by about 3 per cent of a free fall time, or about 17.7 kyr. Major heating of the gas lagged by about 1 per cent of a free fall time, or about 5.9 kyr. The difference in heating and ionization was due to the fact that in Peters et al. (2010a), the stellar radius was underestimated (a ZAMS-equivalent value was taken), when protostars have radii an order of magnitude larger than a ZAMS star of equal mass. The correspondingly higher surface temperatures resulted in excess heating and ionization in this model. When both models had stars converging on to the main sequence, the differences between the two models diminished.

It is possible that these initial differences could have had a lasting effect on the stellar population. The most massive star at the end of each simulation was $43.5\,M_{\odot}$ in the evolving protostar model, and $47.3\,M_{\odot}$ in the Peters et al. (2010a) case – a difference of 8 per cent. The differences in mass between the most massive star and the next largest star was $7.5\,M_{\odot}$ in the evolving protostar case and $14\,M_{\odot}$ in the Peters et al. (2010a) case. It would require further simulations, varying the initial conditions, to confirm that this is always the case.

The cluster of stars is embedded in a rotating disc of gas approximately 0.2 pc in size. The expanding H II regions above and below the disc are rapidly changing in shape and size on time-scales shorter than 570 yr. The physical size of these H II regions in our simulation is at most about 0.2 pc. This flickering is observed regardless of the pre-stellar model used.

Future simulations will have initial conditions including turbulence to model molecular clouds as realistically as possible. The stars will no longer be forming within a global disc, but rather along sheets and filaments in diverse parts of the cloud. With star formation thus spread out more in space and time, we expect the influence of individual young stellar objects on their environments to be more significant than when all stars form in a central cluster. It will be important to have the radiative feedback accurately modelled in these cases.

ACKNOWLEDGMENTS

We thank Mark Krumholz for clarifying some of the more technical aspects of the protostellar evolution method employed in the ORION code and described in Offner et al. (2009). This was very helpful in developing the FLASH module following the same method. We thank Takashi Hosokawa for sharing data from Hosokawa & Omukai (2009) with us. We also thank our anonymous referee for a very careful review of our paper that helped to significantly clarify the presentation of our results. MK acknowledges financial support from the Ontario Graduate Scholarship Program. REP is supported by a Discovery Grant from the Natural Sciences and Engineering Research Council (NSERC) of Canada. TP acknowledges financial support as a Fellow of the Baden-Württemberg Stiftung funded by their program International Collaboration II (grant P-LS-SPII/18) and through SNF grant 200020_137896. The FLASH code was in part developed by the DOE-supported Alliances Center for Astrophysical Thermonuclear Flashes (ASCI) at the University of Chicago. This work was made possible by the facilities of the Shared Hierarchical Academic Research Computing Network (SHARCNET: www.sharcnet.ca) and Compute/Calcul Canada.

REFERENCES

Banerjee R., Pudritz R. E., Anderson D. W., 2006, MNRAS, 373, 1091
Banerjee R., Vázquez-Semadeni E., Hennebelle P., Klessen R. S., 2009, MNRAS, 398, 1082
Bate M. R., 2009, MNRAS, 392, 1363
Beuther H., Churchwell E. B., McKee C. F., Tan J. C., 2007, in Reipurth B., Jewitt D., Keil K., eds, Protostars and Planets V. Univ. Arizona Press, Tucson, p. 165
Blitz L., 1993, in Levy E. H., Lunine J. I., eds, Protostars and Planets III. Univ. Arizona Press, Tucson, p. 125
Clarke C. J., Bonnell I. A., Hillenbrand L. A., 2000, in Mannings V., Boss A. P., Russell S. S., eds, Protostars and Planets IV. Univ. Arizona Press, Tucson, p. 151
Evans N. J., II, 1999, ARA&A, 37, 311
Federrath C., Banerjee R., Clark P. C., Klessen R. S., 2010, ApJ, 713, 269
Franco-Hernández R., Rodríguez L. F., 2004, ApJ, 604, L105
Fryxell B. et al., 2000, ApJS, 131, 273
Galván-Madrid R., Rodríguez L. F., Ho P. T. P., Keto E., 2008, ApJ, 674, L33
Galván-Madrid R., Peters T., Keto E. R., Mac Low M.-M., Banerjee R., Klessen R. S., 2011, MNRAS, 416, 1033
Gómez L., Rodríguez L. F., Loinard L., Lizano S., Allen C., Poveda A., Menten K. M., 2008, ApJ, 685, 333
Hoare M. G., Kurtz S. E., Lizano S., Keto E., Hofner P., 2007, in Reipurth B., Jewitt D., Keil K., eds, Protostars and Planets V. Univ. Arizona Press, Tucson, p. 181
Hosokawa T., Omukai K., 2009, ApJ, 691, 823
Iliev I. T. et al., 2006, MNRAS, 371, 1057
Keto E., 2002, ApJ, 580, 980
Keto E., 2003, ApJ, 599, 1196
Keto E., 2007, ApJ, 666, 976
Krumholz M. R., Matzner C. D., 2009, ApJ, 703, 1352
Krumholz M. R., Klein R. I., McKee C. F., 2007, ApJ, 656, 959
Krumholz M. R., Cunningham A. J., Klein R. I., McKee C. F., 2010, ApJ, 713, 1120
Krumholz M. R., Klein R. I., McKee C. F., 2011, ApJ, 740, 74
Matzner C. D., 2002, ApJ, 566, 302
McKee C. F., Tan J. C., 2003, ApJ, 585, 850
Mezger P. G., Henderson A. P., 1967, ApJ, 147, 471
Murray N., Ménard B., Thompson T. A., 2011, ApJ, 735, 66
Nakano T., Hasegawa T., Norman C., 1995, Ap&SS, 224, 523
Nakano T., Hasegawa T., Morino J.-I., Yamashita T., 2000, ApJ, 534, 976
Offner S. S. R., Klein R. I., McKee C. F., Krumholz M. R., 2009, ApJ, 703, 131
Palla F., Stahler S. W., 1991, ApJ, 375, 288
Palla F., Stahler S. W., 1992, ApJ, 392, 667
Paxton B., 2004, PASP, 116, 699
Peters T., Banerjee R., Klessen R. S., Mac Low M.-M., Galván-Madrid R., Keto E. R., 2010a, ApJ, 711, 1017
Peters T., Klessen R. S., Mac Low M.-M., Banerjee R., 2010b, ApJ, 725, 134
Peters T., Mac Low M.-M., Banerjee R., Klessen R. S., Dullemond C. P., 2010c, ApJ, 719, 831
Peters T., Banerjee R., Klessen R. S., Mac Low M.-M., 2011, ApJ, 729, 72
Pollack J. B., Hollenbach D., Beckwith S., Simonelli D. P., Roush T., Fong W., 1994, ApJ, 421, 615
Rijkhorst E.-J., Plewa T., Dubey A., Mellema G., 2006, A&A, 452, 907
Rodríguez L. F., Gómez Y., Tafoya D., 2007, ApJ, 663, 1083
Spitzer L., 1978, Physical Processes in the Interstellar Medium. Wiley Interscience, New York, p. 333
Tan J. C., McKee C. F., 2004, ApJ, 603, 383
Testi L., Sargent A. I., Olmi L., Onello J. S., 2000, ApJ, 540, L53
Tout C. A., Pols O. R., Eggleton P. P., Han Z., 1996, MNRAS, 281, 257
Williams J. P., Blitz L., McKee C. F., 2000, in Mannings V., Boss A. P., Russell S. S., eds, Protostars and Planets IV. Univ. Arizona Press, Tucson, p. 97
Wood D. O. S., Churchwell E., 1989, ApJS, 69, 831
Yorke H. W., Sonnhalter C., 2002, ApJ, 569, 846
Zinnecker H., Yorke H. W., 2007, ARA&A, 45, 481

SUPPORTING INFORMATION

Additional supporting information may be found in the online version of this paper:

Movies. Time evolution of gas density and ionization fraction.

Please note: Wiley-Blackwell are not responsible for the content or functionality of any supporting materials supplied by the authors. Any queries (other than missing material) should be directed to the corresponding author for the paper.

This paper has been typeset from a TEX/LATEX file prepared by the author.